

Indication of intrinsic spin Hall effect in 4d and 5d transition metals

M. Morota,¹ Y. Niimi,^{1,*} K. Ohnishi,¹ D. H. Wei,¹ T. Tanaka,² H. Kontani,² T. Kimura,^{1,†} and Y. Otani^{1,3,‡}

¹*Institute for Solid State Physics, University of Tokyo,
5-1-5 Kashiwa-no-ha, Kashiwa, Chiba 277-8581, Japan*

²*Department of Physics, Nagoya University, Furo-cho, Nagoya 464-8602, Japan*

³*RIKEN-ASI, 2-1 Hirosawa, Wako, Saitama 351-0198, Japan*

(Dated: August 30, 2018)

We have investigated spin Hall effects in 4d and 5d transition metals, Nb, Ta, Mo, Pd and Pt, by incorporating the spin absorption method in the lateral spin valve structure; where large spin current preferably relaxes into the transition metals, exhibiting strong spin-orbit interactions. Thereby nonlocal spin valve measurements enable us to evaluate their spin Hall conductivities. The sign of the spin Hall conductivity changes systematically depending on the number of d electrons. This tendency is in good agreement with the recent theoretical calculation based on the intrinsic spin Hall effect.

PACS numbers: 72.25.Ba, 72.25.Mk, 75.70.Cn, 75.75.-c

I. INTRODUCTION

Spin current, a flow of the spin angular momentum, is an important physical quantity to operate spintronic devices.¹ The spin Hall effect (SHE) is widely recognized as a phenomenon that converts charge current to the spin current requiring neither external magnetic fields nor ferromagnets.²⁻⁴ The search for materials exhibiting large SHEs is therefore a prime task for further advancement of spintronic devices. Since the SHE originates from spin-dependent scattering events, materials with large spin-orbit interactions can be good candidates for efficient generation of the spin current. It is, however, difficult to study the SHEs in such materials since the spin diffusion length is extremely short (of the order of several nanometers). We have established the sensitive electrical detection technique of the SHE using the spin current absorption effect.^{5,6} The greatest advantage of this technique is that one can measure the SHE as well as the spin diffusion length of materials with large spin-orbit interactions on the same device. This enables us to obtain the SH conductivity as well as the SH angle which is defined as the ratio of SH conductivity and charge conductivity.

Spin-dependent Hall effects have been theoretically discussed in terms of two distinct physical mechanisms. One is the extrinsic mechanism induced by the impurity scattering^{7,8} that was intensively investigated a few decades ago as an origin of the anomalous Hall effect (AHE).⁹ The other is the intrinsic mechanism based on the band-structure effect as a manifestation of the Berry phase.^{10,11} It was believed that the intrinsic mechanism is limited only in very clean systems such as semiconductors with high electron mobility.^{12,13} Recently, intrinsic AHEs where spin-orbit interaction together with the interband mixing results in an intrinsic anomalous velocity in the transverse direction have been observed in many systems even at room temperature.¹⁴⁻¹⁸ In the case of SHEs in nonmagnetic materials, on the other hand, there is no Hall voltage since the number of spin-up and down electrons are exactly same. However, when the *pure* spin

current defined as the difference between the spin-up and down currents is injected into such materials, both spin-up and spin-down electrons are scattered to the same side, which can be detected as a Hall voltage. Interestingly, recent theoretical studies show that the magnitude and sign of SH conductivities due to the intrinsic SHE in 4d and 5d transition metals (TMs) change systematically in response to the number of d electrons.¹⁹⁻²² Therefore, systematic experiments of the SHEs in such TMs should help to find the dominant mechanism of the observed SHE.

As described above, the most difficult point for transport measurements of the SHEs in 4d and 5d TMs is their short spin diffusion lengths. The spin absorption technique which is detailed in Refs. 5 and 6 enables us to perform quantitative and systematic studies of the SHEs even in materials with short spin diffusion lengths. In this paper, we report on measurements of the SHEs in various 4d and 5d TMs using the spin absorption technique. The experimentally observed SH conductivities of those TMs are semiquantitatively consistent with the recent calculations based on the intrinsic SHE. This fact strongly supports that the intrinsic mechanism of the SHEs in 4d and 5d TMs is more dominant than the extrinsic ones.

II. EXPERIMENTAL DETAILS

Our device has been fabricated on a thermally oxidized silicon substrate using electron beam lithography on polymethyl-methacrylate (PMMA) resist and subsequent lift-off process. The device is based on the lateral spin valve structure⁶ where a TM middle wire is inserted in between two Permalloy (Py) wires as shown in Fig. 1(a). The Py wires are 30 nm in thickness (t_{Py}) and 100 nm in width (w_{Py}) and have been deposited by means of electron beam evaporation. Here one Py wire (Py1) has large pads at the edges to induce the difference in the switching field. In this work, five different TMs (Nb, Ta, Mo,

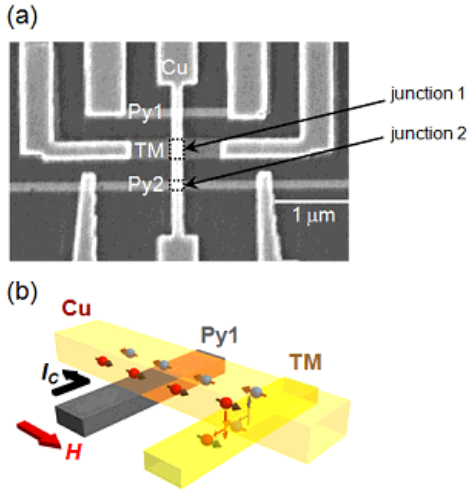


FIG. 1: (Color online) (a) Scanning electron micrograph of a typical spin Hall device consisting of two Py wires and a TM wire bridged by a Cu strip. (b) Schematic of the mechanism of ISHE due to the spin absorption effect.

Pd and Pt) have been used as a middle wire. Nb, Ta and Mo wires were deposited by magnetron sputtering while Pd and Pt wires were grown by electron beam evaporation. The Cu strip whose thickness (t_{Cu}) is 100 nm and whose width (w_{Cu}) is 150 nm was fabricated by a Joule heating evaporator. Prior to Cu evaporation, a careful Ar-ion beam etching was carried out for 30 s to clean the surfaces of Py and TM wires and to obtain highly transparent Ohmic contacts.

When the spin-polarized current is injected from Py1 into the upper side of the Cu strip, there is no net charge current but only a *pure* spin current is induced on the bottom side of the Cu strip [see Fig. 1(b)]. The induced spin current is divided into two segments (TM or the bottom side of Cu strip) at the junction 1 (TM/Cu junction). When the spin relaxation of the TM wire is much stronger than that of the Cu wire, the induced spin current is preferably absorbed into the TM wire. This leads to a drastic reduction of the spin accumulation voltage in the junction 2 (Py2/Cu junction). The flowing direction of the spin current in the TM wire is perpendicular to the plane of junction 1 because of its strong spin-orbit interaction, in other words, its short spin diffusion length.^{5,6} Therefore, the charge accumulation due to the inverse SHE (ISHE) is induced in the TM wire. The measurements have been carried out by using an ac lock-in amplifier and a He flow cryostat. The magnetic field is applied along the easy and hard axes of Py for nonlocal spin valve (NLSV)²³ and ISHE measurements, respectively.

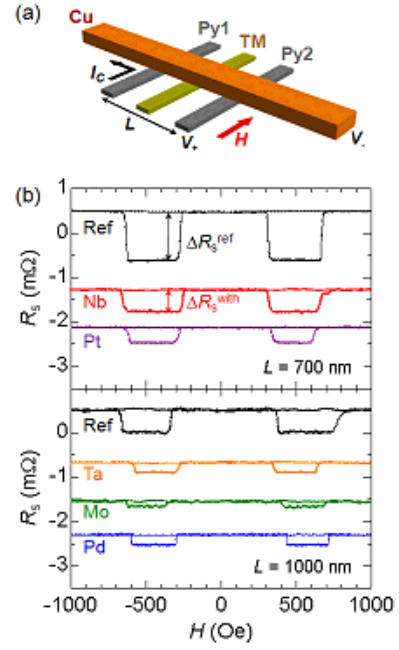


FIG. 2: (Color online) (a) Schematic of the probe configuration for NLSV measurement. (b) NLSV signals R_S with and without TM wires measured at 10 K for $L = 700$ nm (upper panel) and $L = 1000$ nm (lower panel).

III. RESULTS AND DISCUSSION

First, we measure NLSV signals to evaluate the spin diffusion lengths of TM wires as well as the spin current absorbed into the TM middle wires precisely.⁶ As described above, the spin accumulation signal without the TM wires ΔR_S^{ref} ($\equiv \Delta V_S^{\text{ref}}/I_C$, i.e., the spin accumulation voltage divided by the charge current) is reduced to ΔR_S^{with} by inserting the TM middle wires. In Fig. 2(b), we show the NLSV signals for various TM insertions. All the results exhibit clear spin absorption effects, assuring that the spin currents are really absorbed into the TM middle wires via the Cu strip. From the one-dimensional spin-diffusion model proposed by Takahashi and Maekawa,²⁴ the normalized spin accumulation signal $\Delta R_S^{\text{with}}/\Delta R_S^{\text{ref}}$ can be calculated as follows:²⁵

$$\eta \equiv \frac{\Delta R_S^{\text{with}}}{\Delta R_S^{\text{ref}}} \approx \frac{2R_{\text{TM}} \sinh(L/\lambda_{\text{Cu}})}{R_{\text{Cu}}(\cosh(L/\lambda_{\text{Cu}}) - 1) + 2R_{\text{TM}} \sinh(L/\lambda_{\text{Cu}})}. \quad (1)$$

Here R_{Cu} and R_{TM} are the spin resistances for Cu and TM, respectively.²⁶ The spin resistance for Cu is defined by $\frac{\rho_{\text{Cu}} \lambda_{\text{Cu}}}{w_{\text{Cu}} t_{\text{Cu}}}$, where ρ_{Cu} , λ_{Cu} are the electrical resistivity and the spin diffusion length of Cu.²⁴ The spin resistance for TM is defined by $\frac{\rho_{\text{TM}} \lambda_{\text{TM}}}{w_{\text{TM}} w_{\text{Cu}} \tanh(t_{\text{TM}}/\lambda_{\text{TM}})}$, where ρ_{TM} , λ_{TM} , and w_{TM} are the electrical resistivity, the spin diffusion length and the width of the TM wire, respectively. The hyperbolic tangent term comes from the boundary

TABLE I: Device dimensions and some characteristic parameters of various TMs.

Material	w_{TM} (nm)	t_{TM} (nm)	L (nm)	η	λ_{TM} (nm)	σ_{TM} ($10^3 \Omega^{-1} \text{cm}^{-1}$)	σ_{SHE} ($10^3 \Omega^{-1} \text{cm}^{-1}$)	α_{H} (%)
Nb	370	11	700	0.35 ± 0.04	5.9 ± 0.3	11	$-(0.10 \pm 0.02)$	$-(0.87 \pm 0.20)$
Ta	250	20	1000	0.48 ± 0.04	2.7 ± 0.4	3	$-(0.011 \pm 0.003)$	$-(0.37 \pm 0.11)$
Mo	250	20	1000	0.24 ± 0.03	8.6 ± 1.3	28	$-(0.23 \pm 0.05)$	$-(0.80 \pm 0.18)$
Pd	250	20	1000	0.37 ± 0.04	13 ± 2	22	0.27 ± 0.09	1.2 ± 0.4
Pt	100	20	700	0.34 ± 0.03	11 ± 2	81	1.7 ± 0.4	2.1 ± 0.5

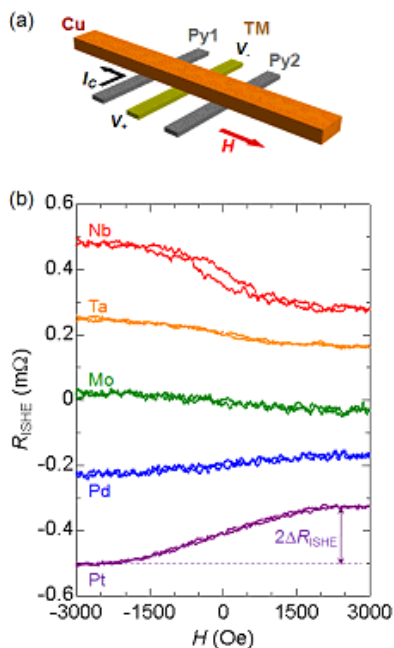


FIG. 3: (Color online) (a) Schematic of the probe configuration for ISHE measurement. (b) ISHE signals measured at 10 K for various TM wires. The device dimensions are shown in Table I.

condition where $I_S = 0$ at the substrate, as detailed in Ref. 27. L is the distance between the two Py wires. Since λ_{Cu} is already known from our previous experiments,²⁸ λ_{TM} can be calculated by using Eq. (1). The spin diffusion lengths λ_{TM} as well as other characteristic parameters for various TM wires are summarized in Table I. In the present study λ_{TM} is quite short for all the TMs, supporting the strong spin-orbit interactions in the TM wires.

Next we measure ISHEs for the TM wires. Note that the direction of the applied magnetic field in this case is parallel to the Cu strip corresponding to the hard axis of the Py wire as shown in Fig. 3(a). In Fig. 3(b) we show the ISHE signals R_{ISHE} measured at 10 K for various TM wires. For all the TM wires, R_{ISHE} linearly changes with the magnetic field below 2000 Oe and saturates above 2000 Oe because the magnetization of the Py wire fully aligns with the direction of the magnetic field. ΔR_{ISHE}

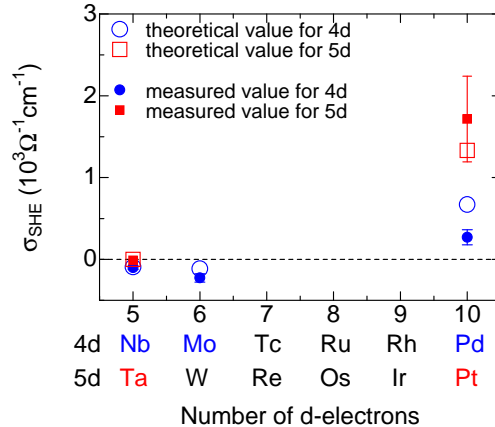


FIG. 4: (Color online) Experimentally measured (closed symbols) and theoretically calculated (open symbols) spin Hall conductivities as a function of the number of d electrons for 4d (circle) and 5d (square) TMs.

defined in this paper is two times smaller than that previously reported by some of the present authors.^{5,6} However, we have adapted the current notation in order to have consistency with AHE measurements, other SHE measurements and theoretical expressions.^{20–22} Interestingly the sign of the slope below 2000 Oe depends on the TMs; the slope is negative for Nb, Ta, and Mo, while it is positive for Pd and Pt. This clearly shows that the sign of the SH conductivity changes depending on the kinds of TMs. A similar material dependence of the sign of SH conductivity has been reported in Refs. 29 and 30, where the spin pumping method has been used to measure ISHEs.

According to the theory on the intrinsic SHE in d -electron systems,²² the SH conductivity in TMs is approximately given by the following equation; $\sigma_{\text{SHE}} \approx (e/4a) \cdot \langle \mathbf{l} \cdot \mathbf{s} \rangle / \hbar^2$, where a and $\langle \mathbf{l} \cdot \mathbf{s} \rangle$ are the lattice constant and the expectation value of the LS coupling, respectively. From the Hund's third rule, $\langle \mathbf{l} \cdot \mathbf{s} \rangle$ is negative (positive) when the number of electrons is more (less) than half-filling. The experimentally observed sign change of the SH conductivities in the TM wires is well reproduced by the intrinsic SHE in the d -electron system.

We now discuss the magnitude of the SH conductivities of the TM wires. As mentioned above, the pure spin current is absorbed perpendicularly into the TM wires. This means that the spin current has a distribution along the

thickness direction, i.e., $I_S(z)$ because I_S should vanish at the substrate. The SH conductivity can be calculated by

$$\sigma_{\text{SHE}} = \sigma_{\text{TM}}^2 \frac{w_{\text{TM}}}{x} \left(\frac{I_C}{\bar{I}_S} \right) \Delta R_{\text{SHE}}. \quad (2)$$

where \bar{I}_S is the effective spin current to contribute to ISHE. The factor x is a correction factor taking into account the fact that the horizontal current driven by the ISHE voltage to balance the spin-orbit deflections is partially shunted by the Cu wire above the TM/Cu interface.^{27,31} The correction factor x for each TM is derived

$$\begin{aligned} \frac{\bar{I}_S}{I_C} &\equiv \frac{\int_0^{t_{\text{TM}}} I_S(z) dz}{t_{\text{TM}} I_C} = \frac{\lambda_{\text{TM}} (1 - e^{-t_{\text{TM}}/\lambda_{\text{TM}}})^2}{t_{\text{TM}} (1 - e^{-2t_{\text{TM}}/\lambda_{\text{TM}}})} \frac{I_S(z=0)}{I_C} \\ &\approx \frac{\lambda_{\text{TM}} (1 - e^{-t_{\text{TM}}/\lambda_{\text{TM}}})^2}{t_{\text{TM}} (1 - e^{-2t_{\text{TM}}/\lambda_{\text{TM}}})} \frac{2p_{\text{Py}} R_{\text{Py}} \sinh(L/2\lambda_{\text{Cu}})}{[R_{\text{Cu}} \{\cosh(L/\lambda_{\text{Cu}}) - 1\} + 2R_{\text{Py}} (e^{L/\lambda_{\text{Cu}}} - 1)] + 2R_{\text{TM}} \sinh(L/\lambda_{\text{Cu}})}, \end{aligned} \quad (3)$$

where R_{Py} and p_{Py} are the spin resistance and the spin polarization of Py, respectively. R_{Py} is defined as $\frac{\rho_{\text{Py}} \lambda_{\text{Py}}}{(1-p_{\text{Py}}^2)w_{\text{Py}}w_{\text{Cu}}}$ where ρ_{Py} and λ_{Py} are the electric resistivity and the spin diffusion length of Py.³²

To compare the experimentally obtained SH conductivity with the theoretically calculated value in Ref 21, we plot both of them in Fig. 4. In most cases, the experimental results are quantitatively consistent with the calculated ones within a factor of 2. This fact strongly suggests that the SHEs in 4d and 5d TMs are mainly caused by the intrinsic mechanism as pointed out in Ref 21. Of course, we cannot exclude the possibility of some contributions from the extrinsic mechanisms such as the skew scattering and the side jump. However, we use a pure (at least more than 99.9%) source for each TM and deposit it under a pressure of 10^{-9} Torr. This assures that no other TMs which have d -orbital degrees of freedom and cause large extrinsic SHEs are included, and the resistivity of the TM wire is simply caused by grain boundary, lattice mismatch, other defects and so on. We believe that the contribution from the intrinsic mechanism is more dominant in 4d and 5d TMs than that from the extrinsic one.

In the previous works on the SHE in Pt reported by some of the present authors,^{5,6} the mechanism of the SHE was the extrinsic one (side-jump scattering) and the SH angle (α_{H}) of Pt was 0.37%. In the present study, however, we claim that the dominant mechanism of the SHE in Pt is intrinsic one and the SH angle for Pt is 2.1%, which is about 6 times larger. There are several reasons for our present conclusions; in the previous work,⁶ they concluded that the side-jump mechanism was dominant because the SH resistivity is proportional to ρ_{Pt}^2 . However, this resistivity dependence is also predicted in the

from additional measurements of the resistance of the TM wire with and without the interface with Cu. It is found to be 0.36 ± 0.08 which is not so sensitive to the resistivity within our resistivity range (see supplemental material in Ref. 27). We can obtain ΔR_{SHE} from the ISHE measurements, i.e., $\Delta R_{\text{SHE}} = \Delta R_{\text{ISHE}}$.⁵

In our case, λ_{TM} is always smaller than t_{TM} . The spin currents injected into the TM wire should be diluted in the TM wire, which leads to a smaller ΔR_{ISHE} . To correct this effect, we take into account all the spin currents injected into the TM wire and then divide them by t_{TM} .²⁷

intrinsic mechanism.²⁰⁻²² For the SH angle of Pt, the boundary condition for \bar{I}_S/I_C had not been taken into account appropriately in the previous study (see Eq. (2) in Ref. 6). In the present study, on the other hand, we impose $I_S = 0$ at the bottom of the TM wires. In addition, we consider the shunting effect of the Cu strip as detailed in Ref. 27. The resistivity of the TM wires is much larger than that of the Cu strip ($\rho_{\text{Cu}} = 1.5 \mu\Omega \cdot \text{cm}$). This causes a smaller current flowing the TM wires and as a result causes the underestimation of the SH angle as discussed in Refs. 27 and 31. The SH angle (2.1%) of Pt in the present paper is consistent with that (1.3%) in Ref. 30 and is a few times smaller than that (5.6%) in Ref. 31.

IV. CONCLUSION

In conclusion, we have measured the SH conductivities for various TMs in a lateral spin valve structure. When d electrons are smaller (larger) than the half-filled value, we have observed negative (positive) SH conductivities. Compared to the recent theoretical calculations based on the intrinsic SHEs in 4d and 5d TMs, the experimentally obtained SH conductivities are semiquantitatively consistent with the theoretical ones. This fact strongly indicates that the intrinsic mechanism based on the degeneracy of d -orbitals in the LS coupling is dominant for the SHEs in 4d and 5d TMs.

V. ACKNOWLEDGEMENTS

We acknowledge helpful discussions with J. Inoue, N. Nagaosa, S. Takahashi, and S. Maekawa. We would also like to thank Y. Iye and S. Katsumoto for the

use of the lithography facilities. This work was supported by a Grant-in-Aid for Scientific Research in Priority Area “Creation and Control of Spin Current” (Grant No. 19048013) from the Ministry of Education, Culture, Sports, Science and Technology of Japan.

-
- * Electronic address: niimi@issp.u-tokyo.ac.jp
 † Present address: Inamori Frontier Research Center, Kyushu University, 744 Motoooka, Nishi-ku, Fukuoka 819-0395, Japan
 ‡ Electronic address: yotani@issp.u-tokyo.ac.jp
- ¹ S. Maekawa, *Nature Mater.* **8**, 777 (2009).
 - ² M. I. Dyakonov, *Int. J. Mod. Phys. B*, **23**, 2556 (2009).
 - ³ J. E. Hirsch, *Phys. Rev. Lett.* **83**, 1834 (1999).
 - ⁴ S. Zhang, *Phys. Rev. Lett.* **85**, 393 (2000).
 - ⁵ T. Kimura, Y. Otani, T. Sato, S. Takahashi, and S. Maekawa, *Phys. Rev. Lett.* **98**, 156601 (2007).
 - ⁶ L. Vila, T. Kimura, and Y. Otani, *Phys. Rev. Lett.* **99**, 226604 (2007).
 - ⁷ J. Smit, *Physica (Amsterdam)* **24**, 39 (1958).
 - ⁸ L. Berger, *Phys. Rev. B* **2**, 4559 (1970).
 - ⁹ A. Fert and O. Jaoul, *Phys. Rev. Lett.* **28**, 303 (1972).
 - ¹⁰ R. Karplus and J. M. Luttinger, *Phys. Rev.* **95**, 1154 (1954).
 - ¹¹ N. Nagaosa, *J. Phys. Soc. Jpn.* **75**, 042001 (2006).
 - ¹² S. Murakami, N. Nagaosa, S.-C. Zhang, *Science* **301**, 1348 (2003).
 - ¹³ J. Sinova, D. Culcer, Q. Niu, N. A. Sinitsyn, T. Jungwirth, and A. H. MacDonald, *Phys. Rev. Lett.* **92**, 126603 (2004).
 - ¹⁴ W.-L. Lee, S. Watauchi, V. L. Miller, R. J. Cava, and N. P. Ong, *Science* **303**, 1647 (2004).
 - ¹⁵ T. Miyasato, N. Abe, T. Fujii, A. Asamitsu, S. Onoda, Y. Onose, N. Nagaosa, and Y. Tokura, *Phys. Rev. Lett.* **99**, 086602 (2007).
 - ¹⁶ Y. Tian, L. Ye, and X.-F. Jin, *Phys. Rev. Lett.* **103**, 087206 (2009).
 - ¹⁷ S. Onoda, N. Sugimoto and N. Nagaosa, *Phys. Rev. Lett.* **97**, 126602 (2006).
 - ¹⁸ In Ref. 17, the extrinsic term is more dominant in the clean regime than the intrinsic one, which seems to be inconsistent with Refs. 12 and 13. However, the extrinsic term strongly depends on the property of impurity, in other words, its orbital degrees of freedom as detailed in Ref. 20. In this sense, the statement about the extrinsic term in Ref. 17 is not general.
 - ¹⁹ G. Y. Guo, S. Murakami, T.-W. Chen, and N. Nagaosa, *Phys. Rev. Lett.* **100**, 096401 (2008).
 - ²⁰ H. Kontani, M. Naito, D. S. Hirashima, K. Yamada, and J. Inoue, *J. Phys. Soc. Jpn.* **76**, 103702 (2007).
 - ²¹ T. Tanaka, H. Kontani, M. Naito, T. Naito, D. S. Hirashima, K. Yamada and J. Inoue, *Phys. Rev. B* **77**, 165117 (2008).
 - ²² H. Kontani, T. Tanaka, D. S. Hirashima, K. Yamada, and J. Inoue, *Phys. Rev. Lett.* **102**, 016601 (2009).
 - ²³ See, for example, Y. Otani and T. Kimura, *Physica E* **43**, 735 (2011).
 - ²⁴ S. Takahashi and S. Maekawa, *Phys. Rev. B* **67**, 052409 (2003).
 - ²⁵ Equation (1) in the present paper is different from Eq. (1) in Ref. 6 by a factor of 2 in front of the hyperbolic sine term. In the present manuscript we take into account only one path for spin relaxation whose direction is perpendicular to the plane of the TM middle wires. On the other hand, in Ref. 6 there are two paths for the spin relaxation, i.e., side edges of the TM wires. Since the spin diffusion lengths of the TM wires are extremely small, spin current should be absorbed perpendicularly into the plane of the TM wires, not from the side edges. It is known that the former model gives a better fitting for the distance dependence of NLSV than the latter one (see Ref. 28).
 - ²⁶ The spin resistance defined here is expressed by $\rho\lambda/A$. This means that a larger spin resistance corresponds to less spin diffusion process, which is intuitively opposite to a normal resistance.
 - ²⁷ Y. Niimi, M. Morota, D. H. Wei, C. Deranlot, M. Basletic, A. Hamzic, A. Fert, and Y. Otani, *Phys. Rev. Lett.* **106**, 126601 (2011).
 - ²⁸ T. Kimura, T. Sato and Y. Otani, *Phys. Rev. Lett.* **100**, 066602 (2008).
 - ²⁹ O. Mosendz, J. E. Pearson, F. Y. Fradin, G. E. W. Bauer, S. D. Bader and A. Hoffmann, *Phys. Rev. Lett.* **104**, 046601 (2010).
 - ³⁰ O. Mosendz, V. Vlaminck, J. E. Pearson, F. Y. Fradin, G. E. W. Bauer, S. D. Bader, and A. Hoffmann, *Phys. Rev. B* **82**, 214403 (2010).
 - ³¹ L. Liu, T. Moriyama, D. C. Ralph, and R. A. Buhrman, *Phys. Rev. Lett.* **106**, 036601 (2011)
 - ³² ρ_{PY} , p_{PY} λ_{PY} are $19 \mu\Omega\text{-cm}$, 0.23 and 5 nm at 10 K , respectively.